

In silico design and molecular docking study of some novel flutamide analogues in the management of prostate cancer

Ajay Kumar Gupta¹, Achal Mishra² and Sanmati Kumar Jain^{1,*}

¹Drug Discovery and Research Laboratory, Department of Pharmacy, Guru Ghasidas Vishwavidyalaya (A Central University), Bilaspur 495 009, India

²Shri Shankaracharya Institute of Pharmaceutical Sciences and Research, Shri Shankaracharya Technical Campus, Durg 490 020, India

The androgen receptor (AR) plays a crucial role in the development of sexual functions in men, as well as the overexpression of androgenic hormones that contribute to prostate cancer (PC) development. Therefore, AR is an essential target for PC research. The aryl group of flutamide has been used as a replacement site in the present study to design newer and safer analogues using a bioisosteric approach with reduced toxicity. To design flutamide analogues, MolOpt was used along with ADMETlab 2.0 to determine their pharmacokinetic and toxicity properties. Additionally, OSIRIS Property Explorer was used to eliminate drug-likeness and drug score. Docking of the newly designed analogues was carried out using ArgusLab 4.0.1 based on Hartree–Fock calculations. The docking score ranged from –8.12 to –11.06 kcal/mol for all the ligands. A good binding score was observed for ligands 008, 009, 012, 016, 018 and 020, which had significantly better binding features than the other ones. Results from the *in silico* approaches (docking and ADMET study) suggest that these compounds 008 and 020 may have the potential as anti-androgen for prostate cancer. The hypothesis may be tested by synthesizing and evaluating the compounds for anti-androgen activity using *in vitro* and *in vivo* approaches.

Keywords: Anti-androgen agent, bioisosteric approach, flutamide, molecular docking, prostate cancer.

ACCORDING to the Globocan 2020 estimates released by the International Agency for Research on Cancer, Lyon, France, there would occur about 19.3 million new cancer cases worldwide, while almost 10.0 million people will die from the disease in 2020. The number of new prostate cancer (PC) patients was 1.4 million (7.3%), while the number of deaths was almost 3.8 million (ref. 1). The androgen receptor (AR) is a type of nuclear receptor which is responsible for sexual development of the male reproductive system. Testosterone and hydroxytestosterone are two endogenous androgens which give their biological response by binding with AR^{2–4}. The proliferation of prostate cells is enhanced by androgens such as testosterone and hydroxytestosterone⁵.

AR is divided into three domains: the DNA-binding domain (DBD), the ligand-binding domain (LBD) and the N-terminal domain (NTD). DBD and LBD are involved in the translocation of AR from the cytoplasm to the nucleus, whereas NTD contains amino acids like polyglutamine and polyglycine to regulate transcription⁶. As a result of the overexpression of AR, testosterone may be transported more readily into tumour cells, causing DNA transcription and proliferation, which may lead to PC. Currently, PC is treated by a single or combination of approaches, including castration (removal of the testicles), radiation implant and hormonal treatment (AR antagonists). The disease is treated with flutamide, bicalutamide and nilutamide. These treatments become resistant to the AR antagonists after 2–4 years because of mutation in the AR^{7,8}.

Flutamide is a nonsteroidal antiandrogen drug which is chemically 2-methyl-*N*-[4-nitro-3-(trifluoromethyl)phenyl]-propanamide (Figure 1)^{9,10}. It is frequently used to treat PC by blocking the AR after binding and is also effective for the treatment of polycystic ovary syndrome caused by an excess of androgen in women^{11–13}. Recently, it has been used in the treatment of hyperandrogenism in women¹⁴. Flutamide is rapidly absorbed from the oral route, and in the liver, it is converted into the active metabolite 2-hydroxyflutamide (Figure 1)^{15,16}. Idiosyncratic hepatotoxicity can be caused by flutamide due to the formation of metabolites such as 4-nitro-3-(trifluoromethyl)phenylamine and 3-(trifluoromethyl)aniline in the liver microsomes and affects about three out of every 10,000 patients^{17–19}. On the other hand, hepatotoxicity induced by flutamide may be due to the dose, immune response, genetic, or nutrition-related²⁰. Flutamide, a medication commonly used in the

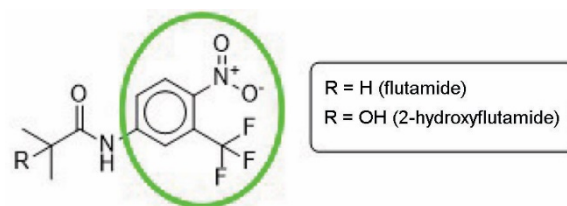


Figure 1. Structure of flutamide and 2-hydroxyflutamide; bioisosteric modification of the aryl group (green circle) in flutamide.

*For correspondence. (e-mail: sanmatijain72@yahoo.co.in)

treatment of prostate cancer, has been associated with potential side effects, including photosensitivity and the ability to cross the placental barrier, raising concerns about its potential impact on fetal development during pregnancy^{21,22}.

Pharmaceutical chemists use bioisosterism as the most common strategy to improve a drug's pharmacokinetic, pharmacodynamic and toxicological profiles. Structures of bioactive compounds share similar molecular volume, shape, electronic distribution and physical–chemical properties. Bioisosteres can be divided into two categories: classical and non-classical. The classical bioisosteres consist of atoms, groups and radicals with the same electrons in the outermost orbital and the same valence. On the other hand, non-classical bioisosteres include groups that are not sterically and electronically similar as in classical bioisosteres. This type of relationship is considered to be the most challenging. The strategies included in bioisosteric approach are retrososterism, ring-opening and ring-closing and equivalent functional groups^{23,24}.

Molecular docking is a type of bioinformatics modeling in which the interaction between ligands and proteins is examined, and the three-dimensional structure of the ligand and protein complex is analysed. Docking estimation of different receptor–ligand interactions may be done using software like Auto Dock, Argus Lab and GOLD. Molecular docking generates various structures of the adducts of proteins and ligands, which are grouped by their scoring function. Docking interactions predict optimized docked conformers based on the total energy of the system. It also helps predict the affinity of the tested molecule with the targeted protein with respect to amino acids of the protein responsible for binding with the test molecules^{25,26}.

In this study, the aryl group has been bioisosterically modified (Figure 1) in the flutamide molecule to develop analogues with lesser side effects, such as hepatotoxicity, than that with the help of absorption, distribution, metabolism, excretion and toxicity (ADMET), drug-likeness (DL), drug score (DS) prediction and docking studies (Figure 1).

Materials and methods

Design of flutamide analogues using the bioisosteric approach

In the treatment of PC, flutamide is used as a pure anti-androgen drug, but it causes hepatotoxicity in the patients. As a result, it is necessary to modify the flutamide structure in order to achieve compounds with less toxic effects. Aryl bioisosteres of flutamide have been generated using MolOpt²⁷ (Table 1). Data mining, deep generation and similarity comparison are used in this *in silico* tool for bioisosteric transformation. Navigating the historical bioisosteric group space can also give ideas for bioisosteric transformation.

Pharmacokinetics and toxicity properties

The ADMET properties of newer flutamide analogues play a vital role in the discovery and development of drugs. A large number of possible candidates fail to become drugs during drug discovery or development. The major reason for drug failure is the lack of efficacy and safety. It is, therefore, necessary to find molecules with better ADMET properties that are efficacious. An *in silico* screening tool, ADMETlab2.0, was used to obtain ADMET profiles for the newly designed analogues^{28–31}. This database contains 84 quantitative and 4 qualitative models that can predict ADMET properties of new molecules in mammals.

Drug likeness and drug score prediction

The DL and DS of the newer analogues of flutamide were determined using OSIRIS Property Explorer (PEO)³². Many approaches are used to predict the DL score in this tool, including topological descriptors, fingerprints of MDL structure keys, molecular weights and clog *P*. DS predictions can be done utilizing descriptors, including DL, clog *P*, log *S*, molecular weight and toxicity risks combined into a single value that may be used to determine the overall potential of a compound as a drug.

Molecular docking studies

Molecular docking plays an important role in drug discovery by identifying interactions of small molecules with the target (receptor). Especially in structure-based drug design, ligand–receptor complexes in receptor-binding sites are important for drug design.

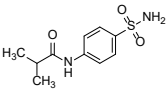
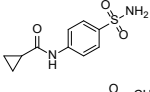
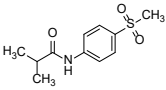
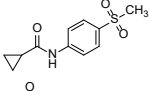
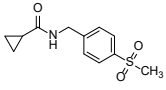
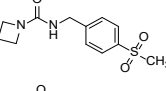
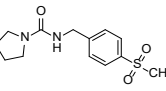
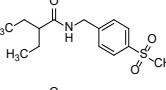
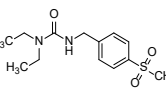
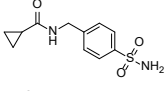
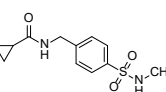
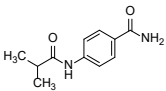
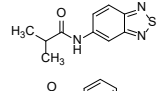
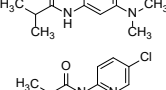
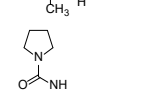
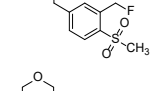
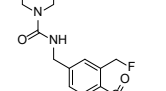
Preparation of protein structure

Docking study was performed with the X-ray structure of the AR modulator (PDB ID: 5T8E). The protein sequence was retrieved in the FASTA format, and the 3D structure was determined using the CPH model server. All water molecules were removed, and hydrogen atoms were added to the target protein molecule.

Preparation of ligand structures

The ligand structures were generated using the ChemDraw software. Three-dimensional optimization of the ligand structures was done, and the result was saved as a '.mol file'. Geometry optimization of the ligands was performed according to the Hartree–Fock (HF) method using ArgusLab 4.0.1 (ref. 33). The compounds included in the study were selected from the newly designed analogues on the basis of ADMET properties for docking calculations³⁴.

Table 1. Structure and molecular properties of the flutamide analogues

Entry no.	Structure	MW	nHA	nHD	nRot	TPSA	log <i>S</i>	log <i>P</i>
001		242.07	5	3	4	89.26	−2.175	0.864
002		240.06	5	3	4	89.26	−2.557	0.411
003		241.08	4	1	4	63.24	−2.332	1.067
004		239.06	4	1	4	63.24	−2.775	0.635
005		253.08	4	1	5	63.24	−2.646	0.319
006		268.09	5	1	5	66.48	−2.102	−0.024
007		282.1	5	1	5	66.48	−2.348	0.4
008		283.12	4	1	7	63.24	−2.809	1.756
009		284.12	5	1	7	66.48	−2.295	0.777
010		254.07	5	3	5	89.26	−2.398	−0.01
011		268.09	5	2	6	75.27	−2.425	0.701
012		206.11	4	3	4	72.19	−2.211	1.11
013		221.06	4	1	3	54.88	−3.124	2.363
014		206.14	3	1	4	32.34	−2.459	2.48
015		198.06	3	1	2	45.22	−1.809	1.987
016		314.11	5	1	6	66.48	−2.43	0.641
017		330.1	6	1	6	75.71	−2.157	−0.045

(Contd)

Table 1. (Contd)

Entry no.	Structure	MW	nHA	nHD	nRot	TPSA	log <i>S</i>	log <i>P</i>
018		316.13	5	1	8	66.48	−2.344	0.957
019		287.1	4	1	6	63.24	−2.232	0.984
020		285.08	4	1	6	63.24	−2.596	0.582
021		300.09	5	1	6	66.48	−2.186	0.257
022		231.02	2	1	3	29.1	−4.373	3.706
023		222.06	3	1	3	52.89	−4.062	2.766
024		313.99	3	1	3	52.89	−4.579	3.148
025		202.11	3	1	3	52.89	−3.963	2.659
026		238.11	3	1	3	52.89	−5.105	2.982
027		264.98	2	1	3	29.1	−5.478	4.351
028		247.16	3	1	5	38.33	−4.906	3.63
029		177.12	2	1	4	29.1	−1.552	1.908
030		187.12	4	1	7	55.4	−0.355	0.722
031		173.11	4	1	6	55.4	−0.734	0.65
032		143.13	2	1	5	29.1	−0.922	1.68
033		256.09	5	3	5	89.26	−1.856	0.626
034		242.07	5	3	5	89.26	−1.921	0.11
Flutamide		276.07	5	1	5	72.24	−3.842	3.243

MW, Molecular weight; nHA, Number of hydrogen-bond acceptors; nHD, Number of hydrogen-bond donors; nRot, Number of rotatable bonds; TPSA, Topological polar surface area; log *P*, Logarithm of the *n*-octanol/water distribution coefficient; log *S*, Logarithm of the aqueous solubility value.

Table 2. Medicinal properties of the selected analogues

Entry no.	QED	Synth	Fsp3	MCE-18	Lipinski	Pfizer	GSK	GT
001	0.826	1.652	0.3	10	Accepted	Accepted	Accepted	Accepted
002	0.814	1.606	0.3	32	Accepted	Accepted	Accepted	Accepted
003	0.875	1.615	0.364	10	Accepted	Accepted	Accepted	Accepted
004	0.868	1.57	0.364	31	Accepted	Accepted	Accepted	Accepted
005	0.874	1.642	0.417	31	Accepted	Accepted	Accepted	Accepted
006	0.889	1.758	0.417	31	Accepted	Accepted	Accepted	Accepted
007	0.911	1.773	0.462	31	Accepted	Accepted	Accepted	Accepted
008	0.87	1.903	0.5	10	Accepted	Accepted	Accepted	Accepted
009	0.894	1.898	0.462	10	Accepted	Accepted	Accepted	Accepted
010	0.813	1.675	0.364	31	Accepted	Accepted	Accepted	Accepted
011	0.822	1.743	0.417	31	Accepted	Accepted	Accepted	Accepted
012	0.784	1.525	0.273	8	Accepted	Accepted	Accepted	Accepted
013	0.846	2.161	0.3	11	Accepted	Accepted	Accepted	Accepted
014	0.823	1.739	0.417	8	Accepted	Accepted	Accepted	Accepted
015	0.734	3.348	0.333	7	Accepted	Accepted	Accepted	Rejected
016	0.922	2.313	0.5	33	Accepted	Accepted	Accepted	Accepted
017	0.897	2.395	0.5	33	Accepted	Accepted	Accepted	Accepted
018	0.874	2.444	0.5	11	Accepted	Accepted	Accepted	Accepted
019	0.898	2.329	0.462	11	Accepted	Accepted	Accepted	Accepted
020	0.893	2.254	0.462	32	Accepted	Accepted	Accepted	Accepted
021	0.916	2.331	0.462	32	Accepted	Accepted	Accepted	Accepted
022	0.829	1.569	0.3	8	Accepted	Rejected	Accepted	Accepted
023	0.837	1.876	0.273	8	Accepted	Accepted	Accepted	Accepted
024	0.854	2.243	0.273	8	Accepted	Rejected	Accepted	Accepted
025	0.8	1.911	0.333	8	Accepted	Accepted	Accepted	Accepted
026	0.872	1.888	0.2	12	Accepted	Accepted	Accepted	Accepted
027	0.797	1.955	0.3	9	Accepted	Rejected	Rejected	Accepted
028	0.882	1.755	0.533	26	Accepted	Rejected	Accepted	Accepted
029	0.751	1.38	0.364	6	Accepted	Accepted	Accepted	Rejected
030	0.645	1.794	0.778	0	Accepted	Accepted	Accepted	Rejected
031	0.623	1.807	0.75	0	Accepted	Accepted	Accepted	Rejected
032	0.594	1.674	0.875	0	Accepted	Accepted	Accepted	Rejected
033	0.827	1.747	0.364	10	Accepted	Accepted	Accepted	Accepted
034	0.798	1.707	0.3	9	Accepted	Accepted	Accepted	Accepted
Flutamide	0.68	2.07	0.364	12	Accepted	Rejected	Accepted	Accepted

QED, A measure of drug-likeness based on the concept of desirability; Synth, Synthetic accessibility score; Fsp3, Number of sp³ hybridized carbons/total carbon count; MCE-18, Medicinal chemistry evolution in 2018; GT, Golden triangle.

Protein–ligand docking using ArgusLab 4.0.1

ArgusLab is a program that is based on quantum mechanics. It predicts the potential energy, molecular structure, geometry optimization of a structure, vibration frequency of coordinates of the atoms, bond length and bond angle. The AR modulator (PDB ID: 5T8E) was docked against 22 active compounds using ArgusLab. The interaction was carried out to find the favourable binding geometries of the ligand with the protein. The protein–ligand complex was mainly targeted to the predicted active site. Docking study was performed by selecting ‘ArgusDock’ as the docking engine. The selected residues of the receptor were defined to be a part of the binding site. A spacing of 0.4 Å between the grid points was used, and an exhaustive search was performed by enabling the ‘High precision’ option in the ‘Docking precision’ menu; ‘Dock’ was chosen as the calculation type, ‘flexible’ for the ligand and ‘AScore’ was used as the scoring function. A maximum of 150 poses were allowed

to be analysed; the binding-site box size was set to 20 × 20 × 20 Å so as to encompass the entire active site. The AScore function, with parameters read from the AScore.prm file, was used to calculate the binding energies of the resulting docked structures. All the compounds in the dataset were docked into the active site of the protein using the same protocol. The docking poses saved for each compound were ranked according to their dock score function. The pose having the highest dock score was selected for further analysis.

Results and discussion

Bioisosteres of aryl groups in flutamide

A total of 73 bioisosteres of the aryl group of flutamide were generated, including pyridine, chloropyridine, thiazole, sulphonamide, methane sulphonamide and dimethylamine. Among them, 34 new analogues of flutamide

Table 3. Absorption and distribution profile of the selected analogues

Entry no.	Caco-2	MDCK	BBB	PPB (%)	VDss	Fu (%)	HIA	CYP3A4	CL	$T_{1/2}$
001	-5.112	Ex.	0.497	61.33	0.562	35.99	0.004	+	0.656	0.237
002	-5.268	Ex.	0.644	47.55	0.492	46.24	0.011	+	0.457	0.207
003	-4.849	Ex.	0.723	61.86	0.535	32.28	0.004	+	0.299	0.216
004	-5.168	Ex.	0.841	42.76	0.466	48.83	0.006	+	0.257	0.184
005	-5.115	Ex.	0.639	43.53	0.401	48.72	0.006	+	0.34	0.243
006	-5.552	Ex.	0.638	49.05	0.498	53.38	0.082	+	0.472	0.408
007	-5.435	Ex.	0.669	56.42	0.485	42.00	0.052	+	0.476	0.368
008	-4.731	Ex.	0.509	70.84	0.377	31.27	0.004	+	0.47	0.24
009	-5.005	Ex.	0.573	49.47	0.427	42.87	0.008	+	0.878	0.324
010	-5.228	Ex.	0.209	46.34	0.434	46.85	0.008	+	0.698	0.253
011	-4.958	Ex.	0.07	41.57	0.386	50.17	0.006	+	4.674	0.181
012	-4.952	Ex.	0.998	59.20	0.951	48.13	0.005	+	6.059	0.323
013	-4.639	Ex.	0.957	80.96	1.058	17.28	0.004	+	2.797	0.877
014	-4.324	Ex.	0.953	90.84	1.144	9.76	0.007	+	9.465	0.77
015	-4.462	Ex.	0.99	88.80	0.802	15.97	0.006	+	6.774	0.877
016	-5.386	Ex.	0.691	62.35	0.551	31.62	0.138	+	1.618	0.612
017	-5.427	Ex.	0.327	39.84	0.457	51.09	0.079	+	1.721	0.75
018	-5.068	Ex.	0.504	55.19	0.469	33.31	0.022	+	2.554	0.617
019	-5.031	Ex.	0.679	67.03	0.527	26.46	0.02	+	1.536	0.487
020	-5.172	Ex.	0.772	50.05	0.449	39.36	0.115	+	0.934	0.428
021	-5.442	Ex.	0.645	55.79	0.567	44.29	0.21	+	1.508	0.623
022	-4.282	Ex.	0.876	97.25	1.136	3.38	0.005	+	3.94	0.249
023	-4.343	Ex.	0.916	92.20	0.825	6.84	0.007	+	7.696	0.438
024	-4.349	Ex.	0.931	85.96	0.68	8.50	0.007	+	5.8	0.438
025	-4.393	Ex.	0.918	87.01	0.784	11.08	0.007	-	8.394	0.621
026	-4.356	Ex.	0.777	94.92	0.543	3.35	0.005	-	5.945	0.45
027	-4.371	Ex.	0.515	99.10	2.112	2.30	0.004	+	4.44	0.198
028	-4.39	Ex.	0.38	95.64	0.673	3.25	0.003	-	5.34	0.202
029	-4.253	Ex.	0.837	81.86	0.796	15.3	0.004	+	6.673	0.833
030	-4.419	Ex.	0.886	17.84	0.924	70.21	0.003	+	7.436	0.885
031	-4.408	Ex.	0.936	15.43	0.903	72.71	0.004	+	7.425	0.88
032	-4.287	Ex.	0.904	48.77	1.23	44.14	0.004	+	7.52	0.777
033	-5.077	Ex.	0.184	57.99	0.47	36.48	0.004	+	0.879	0.296
034	-4.893	Ex.	0.074	49.86	0.4	46.39	0.005	+	1.247	0.323
Flutamide	-4.346	Ex.	0.58	95.62	0.832	4.59	0.004	+	4.681	0.237

Caco-2, Human colon adenocarcinoma cell lines; MDCK, Madin–Darby canine kidney cells ($>2 \times 10^{-6}$ cm/s) indicates excellent; HIA, Human intestinal absorption; PPB, Plasma protein binding; BBB, Blood–brain barrier; VDss, Volume of distribution; Fu, Fraction unbound in plasma; (-) indicates inhibitor and (+) indicates substrate; CYP3A4, Human cytochrome P450 (isozymes 3A4); CL, Clearance of a drug; $T_{1/2}$, Half-life of a drug; Ex, Excellent.

were selected based on DS, DL and quantitative estimation of druglikeness (QED) values for further studies (molecular docking) (Table 1).

Prediction of molecular properties

It is important to determine the molecular properties of a drug in order to evaluate its DL and DS as a potential drug candidate. Various medicinal properties such as molecular weight (MW), hydrogen acceptor number (nHA), hydrogen donor number (nHD), rotatable bonds number (nRot), topological polar surface area (TPSA), aqueous solubility ($\log S$), partition coefficient ($\log P$), QED and synthetic accessibility score (Synth) of the selected analogues were determined (Table 2). Lipinski's rule of five comprises four criteria based on MW, nHA, nHD and $\log P$. Scores of these criterias are in acceptance unit for newer analogues are as follows, whereas compounds such as 006, 017, 022,

024, 027 and 028 violate $\log P$ property, which is either less or more lipophilic. Furthermore, analogues 008, 009, 012, 016, 018 and 020 adhere to Lipinski's rule of five, indicating proper permeability and bioavailability, and thus might be regarded as drug candidates (Table 1). Newer analogues, such as 022–024 and 026–028, have also been found to violate $\log S$ values, indicating that they are less soluble and have less oral absorption. TPSA was calculated using the surface area occupied by oxygen, nitrogen and hydrogen atoms. In all these cases, the TPSA score was below the range, indicating optimal membrane penetration.

QED scores highlight DL of the new molecules based on their desirability. Analogues with a QED score >0.67 indicate they are suitable drug candidates, whereas flutamide has a QED score of 0.68. It is possible to determine the carbon saturation of molecules using the FSp3 method because small molecules have increased solubility or because of the enhanced 3D features. All analogues showed

Table 4. Toxicity profile, drug likeness and drug score of the selected analogues

Entry no.	H-HT	DILI	Ames	ROA	Carc.	NR-AR	NR-AR-LBD	DL	DS
001	0.235	0.989	0.012	0.268	0.753	0.588	0.051	3.79	0.93
002	0.479	0.986	0.02	0.558	0.85	0.634	0.044	5.42	0.94
003	0.352	0.981	0.012	0.29	0.874	0.012	0.002	2.89	0.9
004	0.477	0.971	0.012	0.592	0.894	0.022	0.002	4.53	0.92
005	0.513	0.94	0.01	0.239	0.564	0.023	0.001	4.86	0.92
006	0.448	0.962	0.01	0.071	0.363	0.038	0.001	4.88	0.93
007	0.386	0.956	0.009	0.095	0.309	0.033	0.001	4.76	0.91
008	0.415	0.924	0.009	0.411	0.185	0.01	0.002	5.16	0.88
009	0.373	0.976	0.011	0.147	0.062	0.016	0.002	5.48	0.92
010	0.463	0.98	0.01	0.278	0.301	0.682	0.019	5.46	0.94
011	0.287	0.815	0.007	0.024	0.104	0.211	0.004	5.42	0.94
012	0.104	0.855	0.012	0.192	0.103	0.157	0.003	2.26	0.89
013	0.953	0.807	0.309	0.104	0.961	0.005	0.003	2.99	0.92
014	0.159	0.847	0.76	0.076	0.822	0.483	0.006	1.95	0.87
015	0.87	0.938	0.052	0.976	0.077	0.081	0.002	0.87	0.78
016	0.859	0.961	0.216	0.979	0.967	0.015	0	2.58	0.85
017	0.841	0.974	0.677	0.948	0.974	0.016	0.001	2.14	0.85
018	0.839	0.972	0.129	0.979	0.924	0.014	0.001	3.29	0.87
019	0.804	0.963	0.081	0.977	0.956	0.008	0.001	0.89	0.76
020	0.791	0.948	0.167	0.947	0.965	0.013	0.001	2.62	0.86
021	0.865	0.965	0.233	0.98	0.968	0.016	0	2.65	0.87
022	0.246	0.917	0.065	0.119	0.158	0.63	0.003	0.14	0.24
023	0.815	0.902	0.26	0.12	0.291	0.776	0.011	-4.14	0.16
024	0.634	0.819	0.123	0.082	0.242	0.764	0.017	-3.84	0.15
025	0.846	0.801	0.479	0.111	0.306	0.739	0.006	-6.19	0.13
026	0.957	0.949	0.907	0.254	0.854	0.801	0.016	-4.83	0.13
027	0.172	0.927	0.042	0.077	0.1	0.727	0.004	0.95	0.24
028	0.44	0.84	0.044	0.418	0.746	0.658	0.004	0.8	0.69
029	0.139	0.129	0.037	0.043	0.035	0.13	0.003	1.47	0.86
030	0.049	0.206	0.035	0.01	0.026	0.038	0.002	-8.4	0.48
031	0.046	0.037	0.011	0.016	0.033	0.176	0.003	-3.52	0.5
032	0.075	0.095	0.024	0.092	0.033	0.024	0.002	-0.19	0.7
033	0.32	0.985	0.008	0.098	0.112	0.668	0.029	3.83	0.93
034	0.28	0.984	0.009	0.053	0.079	0.694	0.103	4.5	0.95
Flutamide	0.578	0.858	0.498	0.067	0.786	0.862	0.018	-12.9	0.16

H-HT, Human hepatotoxicity; DILI, Drug-induced liver injury; Ames, Test for mutagenicity; ROA, Rat oral acute toxicity; NR-AR, Androgen receptor – a nuclear hormone receptor; NR-AR-LBD, Bind with LBD of androgen receptor; DL, Drug likeness; DS, Drug score; Carc, Carcinogenicity.

the desired value (≥ 0.4), with the exception of 007, 009, 019–021, 028 and 030–032. Based upon fragment contributions and complexity penalty, the synthetic accessibility score was designed to estimate the ease of synthesis of drug-like molecules; the results indicated that all the analogues could be synthesized easily. The MCE-18 (medicinal chemistry evolution in 2018) measure is able to score molecules based on their cumulative sp³ complexity. The MCE-18 score gives an idea about novelty of molecule. For flutamide, it was found to be 12. However, the compounds 002, 004–007, 010, 011, 016, 017, 020, 021 and 028 scored above 30, so these analogues may be better. Lipinski, Pfizer, GSK and GT rules if followed, compound may have favourable ADME profile. Analogues such as 008, 009, 012, 016, 018 and 020 were followed it.

Pharmacokinetic and toxicity properties computation

Tables 2 and 3 show the ADMET properties of the newer analogues of flutamide. *In vivo* drug permeability was esti-

mated using human colon adenocarcinoma cell lines (Caco-2). More than 50% of the analogues, such as 001, 002, 004–007, 009, 010, 016–021 and 033, demonstrated excellent permeability through epithelial membranes, indicating eligibility for drug development. MDCK cells were developed for *in vitro* permeability testing. The results showed that all the newer analogues had excellent permeability. Blood–brain barrier (BBB) penetration may lead to the central nervous system (CNS) side effects in the case of drugs with peripheral targets. The analogues 010, 011, 017, 028, 033 and 034 showed permeability in peripheral targets and could not easily cross the BBB, unlike flutamide. During the process of binding to serum proteins, plasma protein binding (PPB) can directly influence oral bioavailability because the free concentration of the drug is at stake. PPB properties of 90% of the analogues were found to be less than 90% compared to flutamide (95%) which indicates compounds may have low therapeutic index. Human intestinal absorption (HIA) is an alternative indicator of oral bioavailability, and the present HIA scores indicate good intestinal absorption.

An important parameter to describe *in vivo* drug distribution is the volume of distribution (VD) that connects the administered dose and initial concentration in the circulatory system. A good volume of distribution was observed for all the analogues. Plasma fraction (Fu) exists in equilibrium between unbound and bound states. All analogues showed good scores for Fu, except 022, 026–028 and flutamide. Approximately two-thirds of the known drugs are metabolized by the human cytochrome P450 (CYP 450), which consists of several isozymes such as 1A2, 3A4, 2C9, 2C19 and 2D6. The analogues might be substrates and inhibitors of CYP3A4. A drug's clearance determines, along with VD, the half-life and, therefore, the frequency of dosing, an important pharmacokinetic parameter. The analogues 012, 014, 015, 023–026 and 028–032 showed moderate clearance, while flutamide showed poor clearance (4.681).

Table 4 shows the toxicity properties such as H-HT, DILI, Ames, ROA, carcinogenicity, NR-AR, NR-AR-LBD. Drug-induced liver injury (DILI) and human hepatotoxicity (H-HT) are important safety concerns for patients and a major reason for drug withdrawals. Drug development programmes will be terminated if a drug shows adverse hepatic effects in clinical trials. The H-HT score of analogues like 001, 011, 012, 014, 022, 027, and 029–034 was 0–0.3, which indicates its safety for patients, while for flutamide it was 0.578 (hepatotoxicity). In contrast, compounds 011 and 013 were found to be less toxic to the liver than flutamide in DILI tests. Analogues 029, 030, 031 and 032 had a lower toxicity level than DILI (less than 0.35). Mutagenicity was used by the Ames test, and the mutagenic effect often correlates with cancer risk. Except for some compounds such as 013, 014, 017, 025, 026 and flutamide, all the newer analogues were non-mutagenic. In order to evaluate the safety of drug candidates, one of the most important steps is to determine the acute toxicity of rats or mice. Results indicated that several newer analogues were free from acute oral toxicity, while some compounds like 002, 004, 008, 015–021 and 028 were moderate to high in toxicity. Carcinogenic chemicals can damage the genome or disrupt cellular metabolic processes. They are also a major cause of drug withdrawal. Some newer analogues are non-carcinogenic, including 008, 009, 011, 012, 016, 022–025, 027 and 029–034. AR is a class of nuclear receptors that plays a major role in PC and other androgen-related diseases. Analogues such as 023–027 were found to interact with AR and might disrupt the endocrine function, inhibit reproduction and interfere with development. Alternatively, all analogues could bind easily to the LBD of AR and show anti-androgen activity.

Drug likeness and drug score prediction

Table 4 shows the DL and DS profiles of the newly designed analogues and their scores. Analogues with higher values

should be considered drug-like candidates. The maximum DL score was found to be more than 5 for ligands 008, 009, 010 and 011. The DL score of the designed analogues was found to be higher than that of flutamide, suggesting that the former are likely to be developed as lead molecules.

Molecular docking studies

The structures of all the ligands were drawn in 2D, converted into 3D, and saved in .mol/PDB format. The ligands were first optimized for docking studies. All the molecular structures of compounds had an affinity to AR, which was optimized for the final docking study.

Protein–ligand interaction using ArgusLab 4.0.1

The molecular docking scores identify the ligands that bind with orientation as observed with AR. Figure 2 is a 3D presentation of the interaction of the ligands with AR.

Table 5. Docking score of the selected analogues

Entry no.	Docking score (kcal/mol)	Bonding of amino acids
001	−9.03112	3383O-877THR, 2.09 Å
002	−9.2597	3383O-877THR, 2.78 Å
003	−9.72223	3383O-877THR, 2.21 Å
004	−10.0166	3383O-877THR, 2.10 Å
005	−10.6346	3383O-877THR, 2.74 Å
006	−8.684	3383O-877THR, 2.89 Å
007	−8.537	540N-708GLY, 2.68 Å
008	−11.069	3383O-877THR, 1.90 Å
009	−10.009	3383O-877THR, 1.977 Å
010	−9.435	1753N-781TYR, 2.900 Å
011	−9.81	1715O-779ARG, 2.898 Å
012	−9.416	3489N-883LYS, 2.123 Å
013	−8.127	1721N-779ARG, 2.928 Å
014	−8.437	549N-711GLN, 2.766 Å
015	−8.70188	1265N-752ARG, 2.214 Å
016	−10.9023	594N-711GLN, 2.899 Å
017	−8.35695	1265N-752ARG, 2.206 Å
018	−10.4406	1161N-746VAL, 2.939 Å
019	−10.4659	3383O-877THR, 2.643 Å
020	−10.7455	3383O-877THR, 2.10 Å
021	−9.34803	1165N-752 RG, 2.339 Å
Flutamide	−9.19558	3383O-877THR, 2.939 Å
		No hydrogen bonds
		3383O-877THR, 2.85 Å
		1265N-752ARG, 2.49 Å
		3383O-877THR, 2.89 Å
		1790O-782SER, 2.44 Å
		1793N-783GLN, 2.92 Å
		1265N-752 ARG, 2.45 Å
		3383O-877THR, 2.25 Å
		1265N-752ARG, 2.99 Å
		1265N-752ARG, 2.82 Å
		3383O-877THR, 2.89 Å
		3378N-877THR, 2.99 Å
		3383O-877THR, 2.47 Å
		1265N-752ARG, 2.43 Å

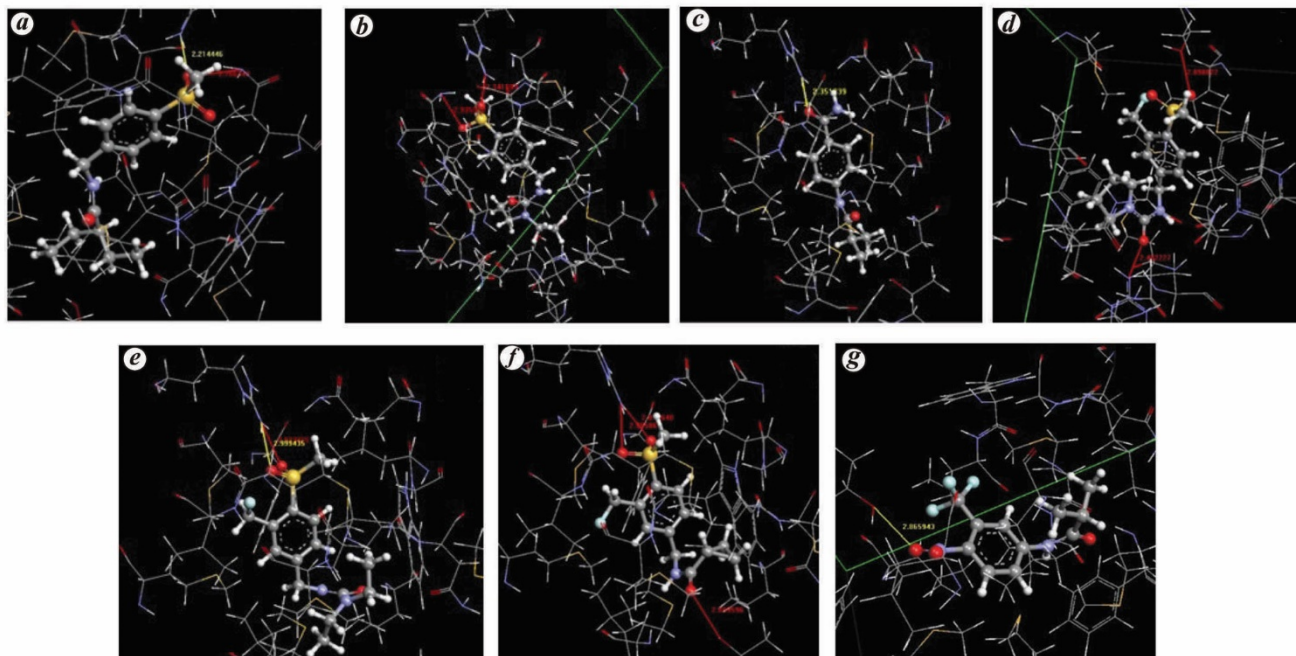


Figure 2. Three-dimensional docking pose of the compounds (a) 008, (b) 009, (c) 012, (d) 016, (e) 018, (f) 020 and (g) flutamide.

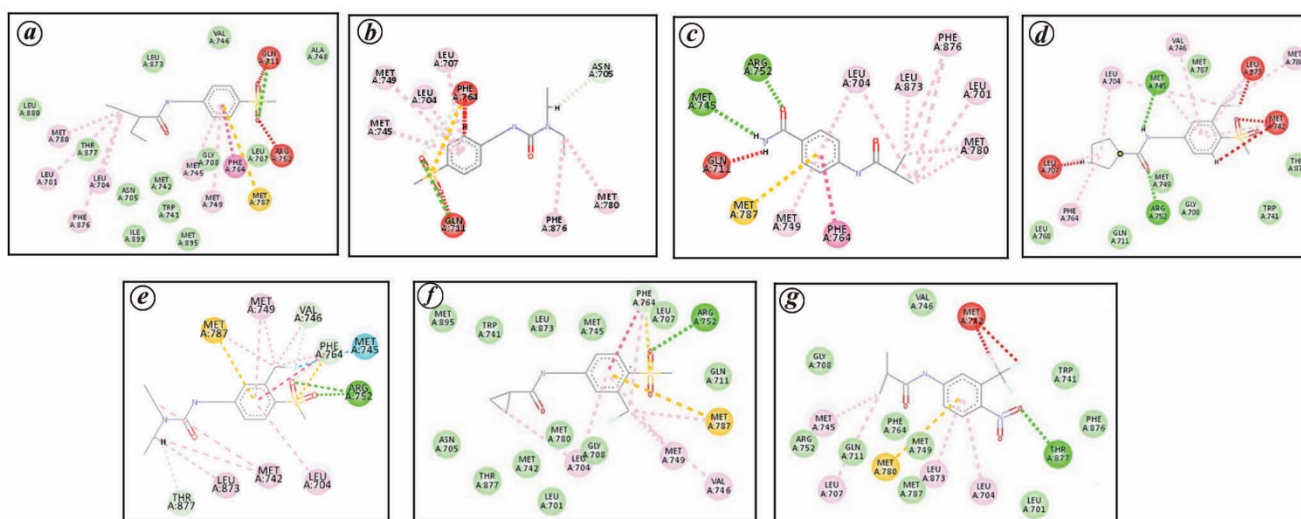


Figure 3. Two-dimensional docking pose of the compounds (a) 008, (b) 009, (c) 012, (d) 016, (e) 018, (f) 020 and (g) flutamide.

All the ligands make good docking poses. The protein–ligand interaction scores (total score) were obtained during docking studies. Table 5 shows the docked poses obtained from visualization and log values of the ligands. The ligands were docked with the target protein, and the best docking poses were identified. Figures 2 and 3 show the 3D and 2D binding poses of the compounds respectively.

The best docking poses show how the ligand molecule fits into the binding region of the target protein. Intermolecular flexible docking simulations were performed, and energy values were calculated from the docked conformations of the AR complex. The majority of the ligands had

a good binding score with the target protein. Interaction was determined by the binding energy of the best ligand pose (kcal/mol). Table 5 lists the binding pose and energy of the analogues. The docking scores of the analogues were found between -8.12 and -11.06 kcal/mol.

All the ligands docked within the binding pocket region, indicating their shape complementarity with the AR. Figure 2 shows a 3D presentation of the docking studies of ligand molecules 008, 009, 012, 016, 018, 020 and flutamide (as standard) with the AR. Most compounds show good docking scores compared to the standard drug flutamide. Compounds like 008, 009, 012, 016, 018 and 020 show higher

docking scores and maximum number of docking poses. The results suggest that these compounds may be potent selective AR inhibitors. Literature suggests that amino acid residue 752ARG forms a hydrogen bond with flutamide analogues. This is important for both binding affinity and antagonist activity³⁵. Results indicated that most compounds formed hydrogen bonds with common amino acid residues like 877THR and 752ARG, which may play a crucial role in binding and antagonistic activity. The residues 704LEU and 745MET formed common pi-alkyl bonding in 008, 016, 020 and flutamide. Compounds 008, 016 and flutamide showed an unfavourable bump (affects the stability of the drug) after docking, while compound 020 did not form any unfavourable bond (Figure 3).

Conclusion

The non-steroidal anti-androgen flutamide is commonly used to treat PC. In this study, the bioisosteric approach was used to design flutamide analogues with fewer side effects than flutamide. Using the *in silico* approach, bioisosteres of the aryl groups in flutamide were generated. A library of 73 bioisosteres was generated using MolOpt. ADMET properties, DL score prediction, DS prediction and docking studies of the newly generated bioisosteres were also carried out. Additionally, some selected analogues were docked with proteins (PDB ID: 5T8E). Several ligands docked well with good binding affinity and orientation. As shown in the molecular docking results, ligands such as 008, 009, 012, 016, 018 and 020 had better binding characteristics to the AR model in terms of energy scores than the other ligands. A hydrogen bond was formed between amino acids 752ARG and 877THR with flutamide analogues, which plays a crucial role in facilitating the antagonistic activity of flutamide analogues. A comparison of the docking scores reveal that the newer analogues, including 008, 009, 012, 016, 018 and 020 may be effective in inhibiting to the AR. All these results from *in silico* approaches (docking and ADMET) suggest that the compounds 008 and 020 may have potential as anti-androgen for PC (docking interactions are comparable with flutamide and its target, PDB ID: 5T8E). This hypothesis may be tested by synthesizing and evaluating the compounds for antiandrogen activity using *in vitro* and *in vivo* approaches.

- Sung, H., Ferlay, J., Siegel, R. L., Laversanne, M., Soerjomataram, I., Jemal, A. and Bray, F., Global cancer statistics 2020: Globocan estimates of incidence and mortality worldwide for 36 cancers in 185 countries. *CA: Cancer J. Clin.*, 2021, **71**, 209–249; <https://doi.org/10.3322/caac.21660>.
- Gunther, J. R., Parent, A. A. and Katzenellenbogen, J. A., Alternative inhibition of androgen receptor signaling: peptidomimetic pyrimidines as direct androgen receptor/coactivator disruptors. *ACS Chem. Biol.*, 2009, **4**(6), 435–440; <https://doi.org/10.1021/cb900043e>.
- Yamada, A., Fujii, S., Mori, S. and Kagechika, H., Design and synthesis of 4-(4-benzoylamino-phenoxy)phenol derivatives as androgen receptor antagonists. *ACS Med. Chem. Lett.*, 2013, **4**(10), 937–941; <https://doi.org/10.1021/ml4001744>.
- Liu, H. L., Zhong, H. Y., Song, T. Q. and Li, J. Z., A molecular modeling study of the hydroxyflutamide resistance mechanism induced by androgen receptor mutations. *Int. J. Mol. Sci.*, 2017, **18**, 1823; <https://doi.org/10.3390/ijms18091823>.
- Stabile, R. G. and Dicks, A. P., Microscale synthesis and spectroscopic analysis of flutamide, an antiandrogen prostate cancer drug. *J. Chem. Educ.*, 2003, **80**(12), 1439–1443; <https://doi.org/10.1021/ed080p1439>.
- Culig, Z., Klocker, H., Bartsch, G. and Hobisch, A., Androgen receptors in prostate cancer. *Endocr. Relat. Cancer*, 2002, **9**(3), 155–170; <https://doi.org/10.1677/erc.0.0090155>.
- He, H. *et al.*, Synthesis and characterization of nonsteroidal-linked $M(CO)_3^+$ ($M = {}^{99m}Tc, Re$) compounds based on the androgen receptor targeting molecule flutamide. *Bioconjug. Chem.*, 2009, **20**(1), 78–86; <https://doi.org/10.1021/bc8003183>.
- Jung, M. E., Ouk, S., Yoo, D., Sawyers, C. L., Chen, C., Tran, C. and Wongvipat, J., Structure–activity relationship for thiohydantoin androgen receptor antagonists for castration resistant prostate cancer (CRPC). *J. Med. Chem.*, 2010, **53**, 2779–2796; <https://doi.org/10.1021/jm901488g>.
- Wen, B., Coe, K. J., Rademacher, P., Fitch, W. L., Monshouwer, M. and Nelson, S. D., Comparison of *in vitro* bioactivation of flutamide and its cyano analogue: evidence for reductive activation by human NADPH: cytochrome P450 reductase. *Chem. Res. Toxicol.*, 2008, **21**(12), 2393–2406; <https://doi.org/10.1021/tx800281h>.
- Trasi, N. S. and Taylor, L. S., Effect of additives on crystal growth and nucleation of amorphous flutamide. *Cryst. Growth Des.*, 2012, **12**, 3221–3230; <https://doi.org/10.1021/cg300370q>.
- Kesavan, G., Pichumani, M. and Chen, S. M., Influence of crystalline, structural, and electrochemical properties of iron vanadate nanostructures on flutamide detection. *ACS Appl. Nano Mater.*, 2021, **4**(6), 5883–5894; <https://doi.org/10.1021/acsnm.1c00802>.
- Caceres, S. *et al.*, *In vitro* and *in vivo* effect of flutamide on steroid hormone secretion in canine and human inflammatory breast cancer cell lines. *Vet. Comp. Oncol.*, 2017, **16**, 148–158; <https://doi.org/10.1111/vco.12324>.
- Niknam, P., Jamehbozorgi, S., Rezvani, M. and Izadkhah, V., Understanding delivery and adsorption of flutamide drug with ZnONS based on: dispersion-corrected DFT calculations and MD simulations. *Phys. E*, 2022, **135**, 114937; <https://doi.org/10.1016/j.physe.2021.114937>.
- Fulghesu, A. M., Melis, F., Murru, G., Canu, E. and Melis, G. B., Very low dose of flutamide in the treatment of hyperandrogenism. *J. Gynaecol. Endocrinol.*, 2018, **34**(5), 394–398; <https://doi.org/10.1080/09513590.2017.1397114>.
- Rojas, P. A., Iglesias, T. G., Barrera, F., Mendez, G. P., Torres, J. and San Francisco, I. F., Acute liver failure and liver transplantation secondary to flutamide treatment in a prostate cancer patient. *Urol. Case Rep.*, 2020, **33**, 33–55; <https://doi.org/10.1016/j.eucr.2020.101370>.
- Shan, J. and Ji, C., Molopt: a web server for drug design using bioisosteric transformation. *Curr. Comput.-Aided Drug Des.*, 2020, **16**(4), 460–466; <https://doi.org/10.2174/157340991566619070409-3400>.
- Kostrubsky, S. E., Strom, S. C., Ellis, E., Nelson, S. D. and Mutlib, A. E., Transport, metabolism, and hepatotoxicity of flutamide, drug–drug interaction with acetaminophen involving phase I and phase II metabolites. *Chem. Res. Toxicol.*, 2007, **20**(10), 1503–1512; <https://doi.org/10.1021/tx7001542>.
- Borse, S., Murthy, Z. V. P., Park, T. J. and Kailasa, S. K., Pepsin mediated synthesis of blue fluorescent copper nanoclusters for sensing of flutamide and chloramphenicol drugs. *Microchem. J.*, 2021, **164**, 105947; <https://doi.org/10.1016/j.microc.2021.105947>.
- Brahm, J., Brahm, M., Segovia, R., Latorre, R., Zapata, R., Ponichik, J., Buckel, E. and Contreras, L., Acute and fulminant

- hepatitis induced by flutamide: case series report and review of the literature. *Ann. Hepatol.*, 2019, **10**(1), 93–98.
20. Coe, K. J. *et al.*, Comparison of the cytotoxicity of the nitroaromatic drug flutamide to its cyano analogue in the hepatocyte cell line TAMH: evidence for complex I inhibition and mitochondrial dysfunction using toxicogenomic screening. *Chem. Res. Toxicol.*, 2007, **20**, 1277–1290; <https://doi.org/10.1021/tx7001349>.
21. Vilapana, J., Romaguera, C., Azon, A. and Lecha, M., Flutamide photosensitivity – residual vitiliginous. *Contact Derm.*, 1998, **38**, 68–70; <https://doi.org/10.1111/j.1600-0536.1998.tb05655.x>.
22. Wiecech, I., Durlej-Grzesiak, M. and Slomczynska, M., Influence of the antiandrogen flutamide on the androgen receptor gene expression in the placenta and umbilical cord during pregnancy in the pig. *Acta Histochem.*, 2013, **115**, 290–295; <https://doi.org/10.1016/j.acthis.2012.08.003>.
23. Lima, L. M. and Barreiro, E. J., Bioisosterism: a useful strategy for molecular modification and drug design. *Curr. Med. Chem.*, 2005, **12**, 23–49; <https://doi.org/10.1016/B978-0-12-409547-2.12290-5>.
24. Kumari, S., Carmona, A. V., Tiwari, A. K. and Trippier, P. C., Amide bond bioisosteres: strategies, synthesis, and successes. *J. Med. Chem.*, 2020, **63**(21), 12290–12358; <https://doi.org/10.1021/acs.jmedchem.0c00530>.
25. Dar, A. M. and Shafia, M., Molecular docking: approaches, types, applications and basic challenges. *J. Anal. Bioanal. Tech.*, 2017, **8**, 1–7; <https://doi.org/10.4172/2155-9872.1000356>.
26. Singh, A. N., Baruah, M. M. and Sharma, N., Structure based docking studies towards exploring potential anti-androgenactivity of selected phytochemicals against prostate cancer. *Sci. Rep.*, 2017, **7**(1), 1955; <https://doi.org/10.1038/s41598-017-02023-5>.
27. Shan, J. and Ji, C., MolOpt: a web server for drug design using bioisosteric transformation. *Curr. Comput.-Aided Drug Des.*, 2020, **16**(4), 460–466; <https://dx.doi.org/10.2174/1573409915666190704-093400>.
28. Xiong, G. *et al.*, ADMETlab 2.0: an integrated online platform for accurate and comprehensive predictions of ADMET properties. *Nucleic Acids Res.*, 2021, **49**, W5–W14; <https://doi.org/10.1093/nar/gkab255>.
29. Dong, J., Wang, N. N., Yao, Z. J., Zhang, L., Cheng, Y., Ouyang, D., Lu, A. and Cao, D., ADMETlab: a platform for systematic ADMET evaluation based on a comprehensively collected ADMET database. *J. Cheminform.*, 2018, **10**(29), 1–11; <https://doi.org/10.1186/s13321-018-0283-x>.
30. Wang, N. *et al.*, ADME properties evaluation in drug discovery: prediction of caco-2 cells permeability using a combination of NSGA-II and boosting. *J. Chem. Inf. Model.*, 2016, **56**(4), 763–773; <https://doi.org/10.1021/acs.jcim.5b00642>.
31. Lei, T., Li, Y., Song, Y., Li, D., Sun, H. and Hou, T., ADMET evaluation on drug discovery: 15. Accurate prediction of rat oral acute toxicity using relevance vector machine and consensus modeling. *J. Cheminform.*, 2016, **8**(6), 1–19; <https://doi.org/10.1186/s13321-016-0117-7>.
32. Sander, T., Freyss, J., von Korff, M., Reich, J. R. and Rufener, C., OSIRIS, an entirely in-house developed drug discovery informatics system. *J. Chem. Inf. Model.*, 2009, **49**(2), 232–246; <https://doi.org/10.1021/ci800305f>.
33. Thompson, M. A., Mark Thompson Planaria software LLC (4.6.2); <http://www.arguslab.com> (accessed on 12 December 2022).
34. Wang, R., Lai, L. and Wang, S., Further development and validation of empirical scoring functions for structure-based binding affinity prediction. *J. Comput. Aided Mol. Des.*, 2002, **16**(1), 11–26; <https://doi.org/10.1023/a:1016357811882>.
35. Suhandi, C., Fadhilah, E., Silvia, N., Atusholihah, A., Prayoga, R. S., Megantara, S. and Muchtaridi, M., Molecular docking study of mangosteen (*Garcinia mangostana* L.) xanthone-derived isolates as antiandrogen. *Int. J. Cancer Chem.*, 2021, **12**(1), 11–20; <https://doi.org/10.14499/indonesianjcanchemprev12iss1pp11-20>.

ACKNOWLEDGEMENT. We thank the Head, Department of Pharmacy, Guru Ghasidas Vishwavidyalaya, Bilaspur for providing the necessary facilities to carry out this work.

Received 16 February 2023; revised accepted 16 October 2023

doi: 10.18520/cs/v126/i4/452-462